Asociación Argentina
de Mecánica Computacional

Mecánica Computacional Vol XXIX, págs. 8981-8993 (artículo completo)
Eduardo Dvorkin, Marcela Goldschmit, Mario Storti (Eds.)
Buenos Aires, Argentina, 15-18 Noviembre 2010

IDENTIFICATION OF STRUCTURAL NONLINEAR DYNAMIC BEHAVIOR OF FLEXIBLE METALLIC COLUMNS UNDER THE ACTION OF SELF-WEIGHT

Daniel L. B. R. Jurjo[a], Carlos Magluta[a], Ney Roitman[a] and Paulo B. Gonçalves[b]

[a]*Civil Engineering Department, Federal University of Rio de Janeiro (COPPE/UFRJ), Rio de Janeiro/RJ, P.O.Box 68506, Brazil, jurjo@coc.ufrj.br, magluta@coc.ufrj.br, roitman@coc.ufrj.br, http://www.coc.ufrj.br*

[b]*Civil Engineering Department, Pontifical Catholic University (PUC-Rio), 22453-900, Rio de Janeiro/RJ, Brazil, paulo@puc-rio.br , http://www.puc-rio.br*

Keywords: Nonlinear dynamic numerical analysis, large deflection behavior, softening phenomenon, dynamic experimental analysis, digital image processing, non-contact displacement measurements.

Abstract. This work presents a numerical and experimental methodologies specially developed for nonlinear free vibration analysis of very flexible structures. In this work, a clamped-free thin-walled metal column under the action of self-weight is investigated. This structure is characterized for presenting, in most cases, highly nonlinear responses, which can not be reproduced by conventional finite-element software due, mainly, to inertial non-linearities caused by the presence of the "softening phenomenon". This phenomenon is related to the loss of stiffness due to the influence of the self-weight together with large rotations, which are inherent to the free vibrations of columns with a high slenderness ratio, leading to important inertial non-linearities. Thus, to overcome this problem, the column is discretized as a sequence of coupled pendulums, retaining the main non-linearities of the problem. The resulting Euler-Lagrange Equations of Motion are solved by the Runge-Kutta integration technique, taking into account the inclusion of the non-linear terms associated to the stiffness of the structural system, aiming to obtain more accurate results, principally, for columns with lengths higher than the critical one. In order to verify the applicability and efficiency of the developed numerical methodology, several experimental free vibration assays were conducted considering the slender metallic column subject to its own weight, in the pre- and post-buckling regimes. As this kind of structure presents a high index of slenderness, its responses can be affected by the introduction of conventional sensors. Therefore, the developed experimental methodology is based on a computer-based vision system that integrates, on-line, the digital image acquisition and its treatment using special image processing techniques. The main characteristic of this methodology is that it performs large displacements measurements without making contact with the structure and thus, not introducing undesirable changes in its behavior, for instance, appreciable changes in mass and stiffness properties. The obtained numerical results presented excellent correlation with the experimental ones, in the pre- and post-buckling regimes, considering the "softening phenomenon".

1 INTRODUCTION

The non-linear effects become increasingly important and difficult to be controlled as the structures become lighter and thinner. The catastrophic collapse of several large structures, anywhere in the world, or the unexpected behavior of certain structures, requiring costly changes in project, reinforcement, or the use of control systems, demonstrate this fact. Besides the presence of the geometrical non-linearity in the modelling of all slender structural element, it also can be taken into account the physical non-linearity, expressed through the stress-strain relations, non-linear damping, non-linear forces (such as from the action of fluids) and non-linearity coming from the boundary conditions (like those from unilateral contact, slacks on the links and non-linear springs, for example, cables used in floating structures). This way, the static and dynamic analysis of non-linear structural systems presents to engineers and researchers a variety of difficult problems solution. So, to solve these kind of problems, it is required the development of sophisticated analysis techniques and knowledge, to learn how the non-linearity affects the structural behavior.

The influence of the self-weight on non-linear dynamic behavior of uni-dimensional slender structures has been a subject of considerable interest in recent years too, mainly due to the increasing slenderness of the structural elements, besides its importance to non-linear mechanics (Jurjo et al. 2010, Gonçalves et al. 2006, Virgin and Plaut 2004). For these structures, the self-weight has a great influence on the geometrically non-linear behavior and stability.

When studying slender elastic uni-dimensional structural elements, the use of strain-displacement linear relationships is not enough. These elements are very flexible, suffering large deflections and rotations. Therefore, it is necessary to use non-linear strain-displacement relationships, which leads to a geometrical non-linear phenomenon.

To represent precisely this kind of structure, a numerical methodology was developed. In this methodology, the structure, in this case a thin-walled column, was modelled as a system with multiple pendulums, as shown in Figure 1. This model aims to represent accurately the large rotations which take place during the column vibration, particularly after its critical buckling length (Lcr). The resulting Euler-Lagrange Equations of Motion from this model were solved by the forth order Runge-Kutta numerical method, which is largely applied due to their usually excellent results (Jurjo 2007, Gonçalves et al. 2006, Pamplona et al. 2001, Jurjo 2001, Anjos 1995, Lee et al. 1993, Wang 1983).

To evaluate the efficiency and accuracy of the numerical methodology in obtaining the dynamic responses, an experimental methodology has also been developed, based on digital image processing techniques (Jurjo et al. 2007, Gonçalves et al. 2006, Hack and Leroy 2005, Yoneyama et al. 2005, Jurjo et al. 2005, Lee and Shinozuka 2006a, Lee and Shinozuka 2006b, Jones et al. 2006). These techniques are rapidly developing, mainly due to the progresses obtained in image acquisition systems and in the development of computers, algorithms and softwares used for general or

specific applications.

The importance of this experimental methodology is that it enables one to perform non-contact displacement measurements, and thus, not introducing undesirable changes in the structure's behavior, since the presence of contact conventional sensors would certainly cause changes in its behavior due to the extreme flexibility (high index of slenderness) inherent in this kind of structure. Taking it into consideration, the proposed experimental methodology only uses adhesive markers of a negligible mass compared to that of the structure, facilitating the implementation of the instrumentation of the experimental test and obtaining more accurate results (Jurjo 2007). This methodology can also be applied to large civil structures, such as bridges and viaducts, where the access for the installation of the conventional instrumentation is usually rather difficult (Lee and Shinozuka 2006a, Lee and Shinozuka 2006b). This is also a promising technique for structures under finite deformations (Jones et al. 2006).

This experimental methodology has been used in an online computer-based vision system, which integrates acquisition and data processing of the images through special programming routines, which make it possible to sharpen the image, identify the adhesive markers (points of interest) and extract their coordinates in the image and convert it all to engineering units.

An inherent advantage of this methodology lies in the low-cost of the developed vision system, comparing to other conventional systems and its similar in the market.

Taking image as a movement sensor, several assays have been done in this work using a clamped-free thin-walled metal column under self-weight in the pre- and post-buckling regimes with different lengths, so that is possible to analyze its non-linear dynamic behavior, in fundamental and post-critical path. This has shown to be a highly cost-effective and easy to implement experimental procedure for the analysis of very flexible structures, and yet maintains the advantage of dynamic measurements with high resolution.

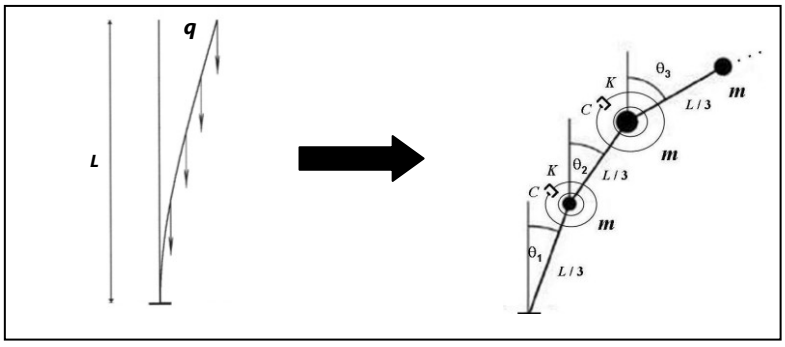

Figure 1 – Column modeling as a sequence of coupled pendulums.

2 EQUATIONS OF MOTION AND COMPUTATIONAL IMPLEMENTATION

To deduce Euler-Lagrange Equations of Motion, it is necessary to obtain the energy functional of the structure. Such functional is given by Lagrange's Function (Lf), shown in Equation (1).

$$Lf = T - \Pi p \tag{1}$$

In Equation (1), quantities T e Πp are, respectively, kinetic and total potential energies of the structure. Kinetic energy is a function of the generalized coordinates, generalized velocities and time. Total potential energy is a function of only generalized coordinates and time (Buffoni 1998).

The structure's total potential energy is given by:

$$\Pi_P = U + V \tag{2}$$

where: U and V are, respectively, the internal strain and the external potential energies.

To the column modeled as a sequence of coupled pendulums, the kinetic and potential energies can be expressed as follows (Braun 2003):

$$T_k = \frac{1}{2} m_k \sum_{i=i}^{k} \sum_{j=1}^{k} l_i l_j \dot{\theta}_i \dot{\theta}_j \cos(\theta_i - \theta_j) \tag{3}$$

$$V_k = m_k g \sum_{i=1}^{k} l_i (1 - \cos\theta_i) \tag{4}$$

where: mk, g, li and lj, θi and θj, $\dot{\theta}_i$ and $\dot{\theta}_j$ are, respectively, masses, gravity acceleration, cord lengths, generalized coordinates and velocities used in the mathematical modeling.

Since the internal strain energy is associated to the springs in the column model, it can be expressed as:

$$U = \frac{1}{2} K \theta_1^2 + \frac{1}{2} K \left[\sum_{i=1}^{k} (\theta_{i+1} - \theta_i)^2 \right] \tag{5}$$

where: K is the elastic constant of the springs.

Manipulating Equations (1), (3), (4) and (5), the energy functional for a sequence of coupled pendulums, as shown in Figure 1, are:

$$L_f = \sum_{k=1}^{n} \left\{ \left[\frac{1}{2} m_k \sum_{i=i}^{k} \sum_{j=1}^{k} l_i l_j \dot{\theta}_i \dot{\theta}_j \cos(\theta_i - \theta_j) \right] - \left[\frac{1}{2} K \theta_1^2 + \frac{1}{2} K \sum_{i=1}^{k} (\theta_{i+1} - \theta_i)^2 \right] - \left[m_k g \sum_{i=1}^{k} l_i (1 - \cos\theta_i) \right] \right\} \tag{6}$$

In Equation (6), n is the number of pendulums used in the modeling.

The Euler-Lagrange Equations of Motion, deduced from Hamilton's Principle (Maia 2000, Clough and Penzien 1993), are:

$$\frac{\partial L}{\partial \theta_i} - \frac{d}{dt}\left(\frac{\partial L}{\partial \dot{\theta}_i} \right) = Q_i \text{ , } i = 1,2, \ldots, n \tag{7}$$

where: Qi are the non-conservative generalized forces, including damping forces.

This way, the equations of motion of the system of n pendulums, in matrix form,

are:

$$\begin{bmatrix} \sum_{i=1}^{n} m_i l^2 & \sum_{i=2}^{n} m_i l^2 \cos(\theta_1-\theta_2) & \sum_{i=3}^{n} m_i l^2 \cos(\theta_1-\theta_3) & \sum_{i=4}^{n} m_i l^2 \cos(\theta_1-\theta_4) \\ \sum_{i=2}^{n} m_i l^2 \cos(\theta_1-\theta_2) & \sum_{i=2}^{n} m_i l^2 & \sum_{i=3}^{n} m_i l^2 \cos(\theta_2-\theta_3) & \sum_{i=4}^{n} m_i l^2 \cos(\theta_2-\theta_4) \\ \sum_{i=3}^{n} m_i l^2 \cos(\theta_1-\theta_3) & \sum_{i=3}^{n} m_i l^2 \cos(\theta_2-\theta_3) & \sum_{i=3}^{n} m_i l^2 & \sum_{i=4}^{n} m_i l^2 \cos(\theta_3-\theta_4) \\ \sum_{i=4}^{n} m_i l^2 \cos(\theta_1-\theta_4) & \sum_{i=4}^{n} m_i l^2 \cos(\theta_2-\theta_4) & \sum_{i=4}^{n} m_i l^2 \cos(\theta_3-\theta_4) & \sum_{i=4}^{n} m_i l^2 \\ & & \vdots & \end{bmatrix} \cdots \begin{bmatrix} \ddot{\theta}_1 \\ \ddot{\theta}_2 \\ \ddot{\theta}_3 \\ \ddot{\theta}_4 \\ \vdots \end{bmatrix} +$$

$$\begin{bmatrix} 0 & \sum_{i=2}^{n} m_i l^2 sen(\theta_1-\theta_2) & \sum_{i=3}^{n} m_i l^2 sen(\theta_1-\theta_3) & \sum_{i=4}^{n} m_i l^2 sen(\theta_1-\theta_4) \\ -\sum_{i=2}^{n} m_i l^2 sen(\theta_1-\theta_2) & 0 & \sum_{i=3}^{n} m_i l^2 sen(\theta_2-\theta_3) & \sum_{i=4}^{n} m_i l^2 sen(\theta_2-\theta_4) \\ -\sum_{i=3}^{n} m_i l^2 sen(\theta_1-\theta_3) & -\sum_{i=3}^{n} m_i l^2 sen(\theta_2-\theta_3) & 0 & \sum_{i=4}^{n} m_i l^2 sen(\theta_3-\theta_4) \\ -\sum_{i=4}^{n} m_i l^2 sen(\theta_1-\theta_4) & -\sum_{i=4}^{n} m_i l^2 sen(\theta_2-\theta_4) & -\sum_{i=4}^{n} m_i l^2 sen(\theta_3-\theta_4) & 0 \\ & & \vdots & \end{bmatrix} \cdots \begin{bmatrix} \dot{\theta}_1^2 \\ \dot{\theta}_2^2 \\ \dot{\theta}_3^2 \\ \dot{\theta}_4^2 \\ \vdots \end{bmatrix} +$$

$$\begin{bmatrix} \sum_{i=1}^{n} glm_i & 0 & 0 & 0 \\ 0 & \sum_{i=2}^{n} glm_i & 0 & 0 \\ 0 & 0 & \sum_{i=3}^{n} glm_i & 0 \\ 0 & 0 & 0 & \sum_{i=4}^{n} glm_i \\ & & \vdots & \end{bmatrix} \cdots \begin{bmatrix} sen\theta_1 \\ sen\theta_2 \\ sen\theta_3 \\ sen\theta_4 \\ \vdots \end{bmatrix} + \begin{bmatrix} 2K & -K & 0 & 0 \\ -K & 2K & -K & 0 \\ 0 & -K & 2K & -K \\ 0 & 0 & -K & K \\ & & \vdots & \end{bmatrix} \cdots \begin{bmatrix} \theta_1 \\ \theta_2 \\ \theta_3 \\ \theta_4 \\ \vdots \end{bmatrix} + \begin{bmatrix} 2C & -C & 0 & 0 \\ -C & 2C & -C & 0 \\ 0 & -C & 2C & -C \\ 0 & 0 & -C & C \\ & & \vdots & \end{bmatrix} \cdots \begin{bmatrix} \dot{\theta}_1 \\ \dot{\theta}_2 \\ \dot{\theta}_3 \\ \dot{\theta}_4 \\ \vdots \end{bmatrix} = \begin{bmatrix} 0 \\ 0 \\ 0 \\ 0 \\ \vdots \end{bmatrix} \tag{8}$$

where: $\ddot{\theta}$ and C are, respectively, the angular acceleration and the damping coefficient.

Equation (8) can be written in a more compact form:

$$RM.\ddot{\theta} + RJ.\dot{\theta}^2 + RW.sen\theta + RK.\theta + RC.\dot{\theta} = 0 \tag{9}$$

where: RM, RJ, RW, RK and RC are, respectively, mass, gyroscopic (anti-symmetrical), gravitational potential, stiffness and damping matrices.

To solve the equations of motion of the modeling, presented in Equation (7), a Fortran implemented Forth-Order Runge-Kutta Algorithm, for a first order ordinary differential equations system, was applied. Thus, displacements, velocities and angular accelerations, for a determined value of n (better range of work: 20 – 50 pendulums) were obtained. From these data, the linear displacement, referring to the free end of the pendulums system, could be determined for each instant.

3 EXPERIMENTAL METHODOLOGY (COMPUTER BASED-VISION SYSTEM)

The proposed experimental methodology encompasses the following steps:

Digitalization: the analogical images captured by the video camera are converted into digital images through a monochromatic digitalization board (frame grabber); (ii) Digital image processing: the quality of the acquired image is enhanced in order to provide a better identification of the image coordinates (u,v) of the centroids of the points of interest. The u and v coordinates of these points are obtained by transforming these points into small regions known in image processing as ROI (Regions of Interest); (iii) Calibration: The purpose of this step is to determine the transformation matrix that correlates the image coordinates and their respective actual coordinates. To obtain the coordinates transformation matrix it is necessary to apply an adequate calibration method. In this study the DLT method is used (Abdel-

Aziz and Karara 1971); (iv) Reconstruction: This step consists in obtaining the actual coordinates by using the transformation matrix and the image coordinates. In this way, it is possible to obtain the actual position of the points of interest and compute the displacements without making contact with the structure.

From these steps, a computational vision system, based on the programming language LabVIEW, which deals with, in real time, the acquisition and the processing of the digital image was developed. The program is named Image-Sensor Program (ISP). Additionally, this system allows the adjustments of the camera, such as zoom, focus, image capture mode (frame or field), among other functions, to be performed via programming. The camera used in this study has analogical video signals, the same used by television. The image capture mode applied in this work is based on a non-interlinked analogical video signal, denominated field. In this mode, the image is composed of a single field, even or odd, with a time interval between them of 1/60s. The field mode results in an image with half of the height, and twice the capture frequency of the frame mode (30 frames/second), i. e., 60 frames/second.

3.1 DLT Method

The DLT method uses the co-linearity equation (Haralick and Shapiro 1993) to express the relation between the image coordinates (u, v) and its respective actual ones (x, y) in the plane, that is, each actual point and its respective image generate a pair of equations, expressed in Equation (1).

$$xL_1 + yL_2 + L_3 - uxL_7 - uyL_8 = u$$

$$xL_4 + yL_5 + L_6 - vxL_7 - vyL_8 = v \tag{10}$$

In Equation (10), the coefficients L1 to L8 are called calibration DLT parameters, which correlate the actual coordinates of a given point in the plane (x, y) to their respective coordinates in the image (u, v). Since the number of unknowns in Equation (10) is equal to eight (DLT parameters), at least 4 points are necessary to calculate the coefficients "Li".

Taking n reference points, the following system is obtained.

$$\begin{bmatrix} x_1 & y_1 & 1 & 0 & 0 & 0 & -u_1x_1 & u_1y_1 \\ 0 & 0 & 0 & x_1 & y_1 & 1 & -v_1x_1 & -v_1y_1 \\ & & & & \vdots & & & \\ x_n & y_n & 1 & 0 & 0 & 0 & -u_nx_n & -u_ny_n \\ 0 & 0 & 0 & x_n & y_n & 1 & -v_nx_n & -v_ny_n \end{bmatrix} \begin{bmatrix} L_1 \\ L_2 \\ \vdots \\ L_7 \\ L_8 \end{bmatrix} = \begin{bmatrix} u_1 \\ v_1 \\ \vdots \\ u_n \\ v_n \end{bmatrix} \tag{11}$$

If n > 4, the system expressed in Equation (11) cannot be directly solved, since it is over-determined. In this case, the problem can be solved using the Least Square Method (LSM), which will search for the best adjustment of the "Li" coefficients from the set of actual and image coordinates, minimizing the errors. The application of the LSM to Equation (11) can be represented as:

$$A_{2n \times 8}.L_{8 \times 1} = B_{2n \times 1} \tag{12}$$

Multiplying both sides of Equation (12) by the transposed of matrix A will result in:

$$C_{8x8}.L_{8x1} = D_{8x1} \tag{13}$$

Manipulating Equation (10) in order to make (x, y) explicit, the following equation is obtained:

$$\begin{bmatrix} L_1^{(1)} - u^{(1)}L_7^{(1)} & L_2^{(1)} - u^{(1)}L_8^{(1)} \\ L_4^{(1)} - v^{(1)}L_7^{(1)} & L_5^{(1)} - v^{(1)}L_8^{(1)} \end{bmatrix} \begin{bmatrix} x \\ y \end{bmatrix} = \begin{bmatrix} u^{(1)} - L_3^{(1)} \\ v^{(1)} - L_6^{(1)} \end{bmatrix} \tag{14}$$

In order to minimize errors in the values of the (x, y) coordinates, this process can be extended to m cameras, through the equations:

$$\underbrace{\begin{bmatrix} L_1^{(1)} - u^{(1)}L_7^{(1)} & L_2^{(1)} - u^{(1)}L_8^{(1)} \\ L_4^{(1)} - v^{(1)}L_7^{(1)} & L_5^{(1)} - v^{(1)}L_8^{(1)} \\ \vdots & \vdots \\ L_1^{(m)} - u^{(m)}L_7^{(m)} & L_2^{(m)} - u^{(m)}L_8^{(m)} \\ L_4^{(m)} - v^{(m)}L_7^{(m)} & L_5^{(m)} - v^{(m)}L_8^{(m)} \end{bmatrix}}_{E} \underbrace{\begin{bmatrix} x \\ y \end{bmatrix}}_{R} = \underbrace{\begin{bmatrix} u^{(1)} - L_3^{(1)} \\ v^{(1)} - L_6^{(1)} \\ \vdots \\ u^{(m)} - L_3^{(m)} \\ v^{(m)} - L_6^{(m)} \end{bmatrix}}_{F}$$

or

(15)

$$E_{2mx2}.R_{2x1} = F_{2mx1} \tag{16}$$

where m is the number of cameras.

Equation (16) results in an over-determined system, which can again be solved by applying the LSM, through the equation:

$$\underbrace{E_{2x2m}^T E_{2mx2}}_{G_{2x2}}.\underbrace{R_{2x1} = E_{2x2m}^T F_{2mx1}}_{H_{2x1}} \tag{17}$$

Once the (u, v) coordinates of the image of the same point in several cameras (at least two cameras) and the "L" coefficients of each one of the cameras are known, their actual coordinates (x, y) can be obtained through the Equation (17).

3.2 Experimental Apparatus

To perform the experimental test, a special apparatus, presented in Figure 2, was developed, where the column, the video camera, the non-oscillating illumination system and the adhesive markers can be seen. A special clamp for the column was designed to enable the variation of the column length during the experiments.

A metallic sheet of brass, representing a slender column, with width b = 9.0 cm; thickness h = 0.45 mm; load per unit length (self-weight) q = 3.43 N/m; Young's Modulus E = 123257 MPa (mean values of the experimental results) and critical length (Lcr): 56.44, was used in the experiments.

The tests were performed with different column lengths, longer (60, 70 cm) and shorter (30, 40, 50 cm) than the critical buckling length (Lcr), enabling an analysis of the dynamic behavior along the fundamental and post-critical equilibrium paths.

In this study, a black background, shown in Figure 2, was used to minimize interferences verified in images acquired with the use of other background colors (Jurjo *et al* 2010). The advantages of the black background are to facilitate the image processing and, particularly, eliminate shadows generated by the column on the background.

To represent the points of interest, the small white rectangular adhesives markers, illustrated in Figure 2, are used. These adhesives are placed along the length of the column at pre-established distances, to obtain the displacements and the deformed shapes of the column at different instants of time. These markers were also placed on the black background, in order to help in the calibration process. Figure 2 also shows the disposition of the points of interest in the columns and in the calibration.

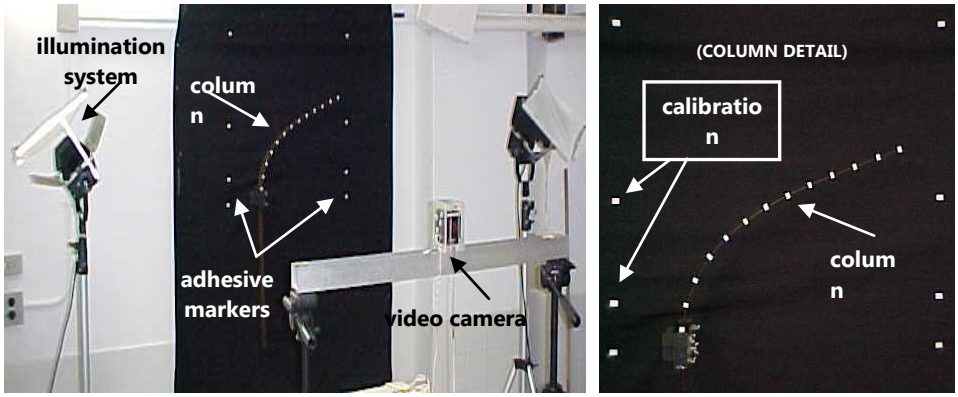

Figure 2 – Apparatus used in the experimental analysis.

To analyze the free vibration responses, the following strategy was adopted: columns with a length smaller than the critical one are subjected to an initial displacement (and null velocity); on the other hand, columns with a length greater than the critical one are released from the vertical unstable equilibrium position. In this case, the column diverges initially from the unstable configuration, presenting a sharp downward movement and, after this, vibrates around the stable post-buckling configuration. For the tensioned configuration, since this configuration is always stable, an initial displacement is imposed to the free end of the column.

As mentioned previously, only one video camera is used with image capture in the field mode. Despite introducing more imprecision in the analysis, this has the advantage of a higher capture frequency (60 frames/s). This frequency became essential in the analysis of the behavior of the column with lengths above the critical one, mainly in the first instants, when the column during the process of divergence from the unstable equilibrium position exhibits large displacements and velocities.

With the use of ISP, the time responses of the x and y coordinates of the markers placed along the column is obtained for all of the analyzed configurations. In this way, it is possible to determine the natural frequencies and damping rates for the different column lengths.

4 RESULTS AND COMMENTS

Figure 3 shows the variation of the displacement at the tip of the column obtained by numerical integration of the equations of motion and the results obtained experimentally, using the ISP, for different column lengths.

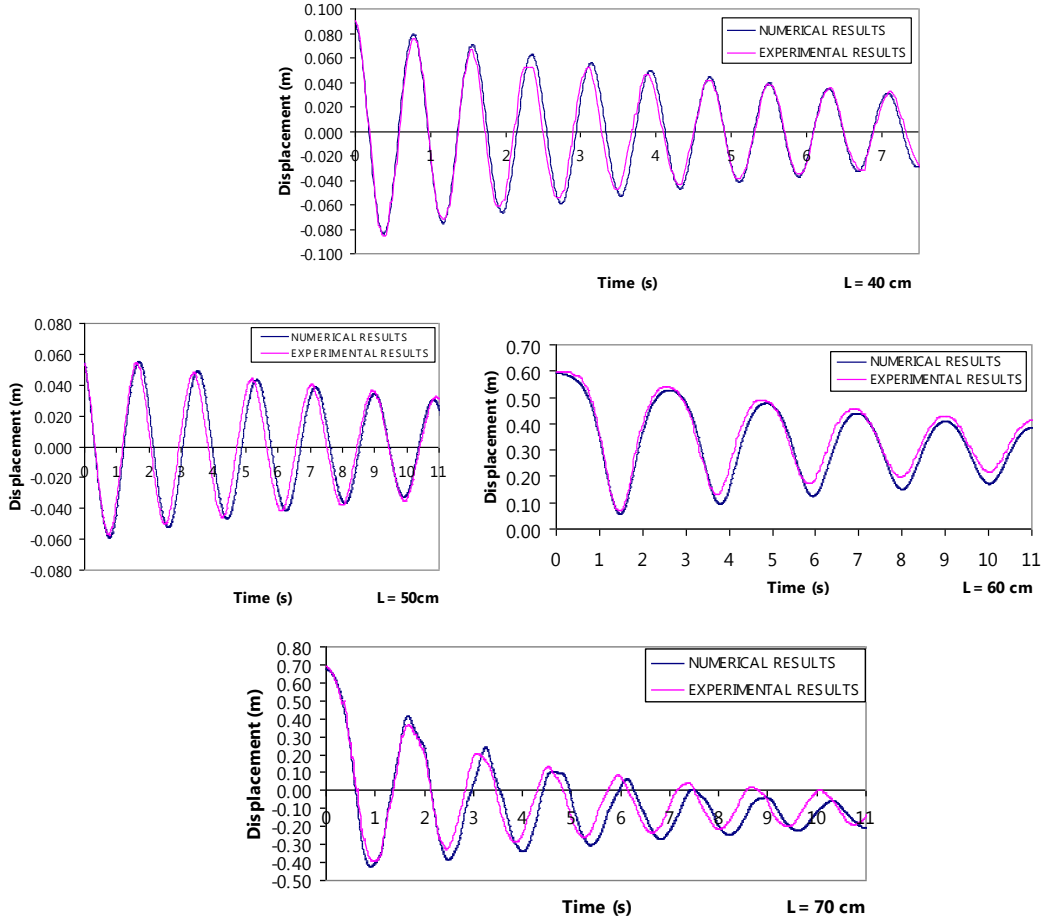

Figure 3 – Comparison between the dynamic responses obtained by the numerical modeling and by the ISP.

From the results presented in Figure 3, it is possible to observe an excellent correlation between numerical and experimental results, assuring the accuracy and the applicability of the methodologies developed in this work, principally, for columns lengths higher than the critical one, where the "softening phenomenon" has a great influence.

It was also verified that the numerical methodology presented in this work was more accurate for the simulation of the "softening phenomenon", on the nonlinear dynamic behavior of the compressed columns, than the methodology based on the application of Rayleigh-Ritz Energy Method using form or approximate functions, which are responsible to represent, in a best way, the deflection curve of the structure (Jurjo 2007).

To obtain more accurate results, principally for columns with lengths higher than

the critical one, it is necessary to represent, in a better way, the stiffness non-linearity of the structure. In the case of the column with length equal to 70 cm (see Figure 3) as can be noted that the numerical methodology has been attended the geometrical and inertial non-linearities, needing to represent with a little more accuracy the stiffness non-linearity of the column. Thus, it would be necessary the inclusion of the non-linear terms associated to the stiffness of the structural system in the Lagrange's Equations of Motion (see Equation 8). The insertion of these non-linear terms in the equations of motion could be done considering the Inextensional Elastica Theory, where the bending moment is proportional to the curvature of the structure, as showed in Equation (18).

$$M = EI * K_{NON-LINEAR} \tag{18}$$

where: E, I and K are, respectively, the Young's Modulus, the moment of inertia and the curvature of the structure. The curvature is expressed by:

$$K_{NON-LINEAR} = \frac{\left(d^2y/dx^2\right)}{[1+(dy/dx)^2]^{3/2}} \tag{19}$$

The function y(x) can be obtained using an approximate equation for the deflection curve of the compressed column. Experimental tests, using the computational vision system and conventional sensors (strain gauges), has been conducted and the numerical simulations are being accomplished, aiming to obtain better dynamic responses taking into account the non-linear terms of the stiffness.

Figure 4 shows the variation of the "instantaneous frequency" as a function of time for a column with L= 50cm.

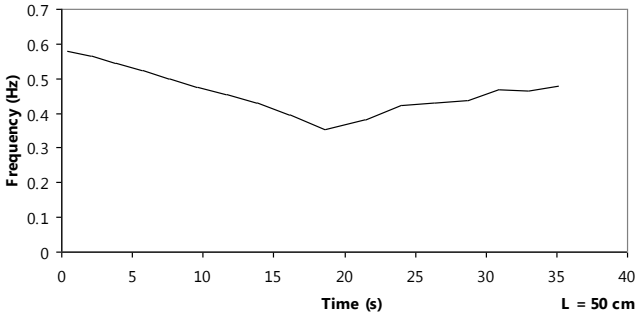

Figure 4 – Natural frequency behavior during the free-vibration movement.

The behavior of the instantaneous natural frequency showed in Figure 4, can be explained from Figure 3, where it can be seen an increase in the vibration period as the free-vibration amplitude decreases, indicating that the column frequency-vibration amplitude is of the softening type. This does not agree with the usual results obtained in literature for slender beams, which are usually of the hardening type (Sathyamoorthy 1998). This behavior of the natural frequency is related to the loss of stiffness due to the influence of the self-weight together with large rotations which are inherent to the free vibrations of columns with a high slenderness ratio. Recently,

Chirikov (Chirikov 2003) also observed a softening phenomenon in the vibration analysis of beams undergoing large rotations.

The comparison between numerical and experimental results, for different lengths of the column, was realized. The results are illustrated in Figure 5.

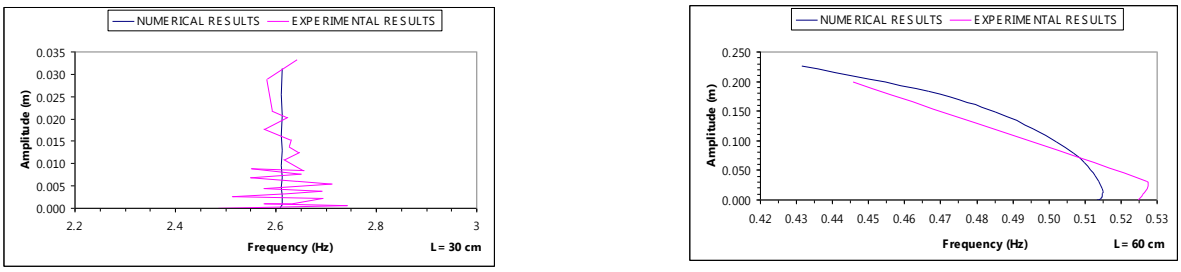

Figure 5 – Natural frequency behavior as a function of the free-vibration movement amplitude.

From the results presented in Figure 5, it is possible to observe a good correlation between numerical and experimental results, for the analyzed column lengths, confirming the efficiency and accuracy of the developed numerical methodology, principally, to the lengths higher than the critical value, where the variation of the natural frequency has a great intensity due to the increase of the "softening phenomenon".

5 CONCLUSIONS

With the use of the numerical modeling and the computer-based vision system, it was possible to obtain, accurately, the dynamic responses of the slender column, for different columns lengths. These developed methodologies also allowed obtaining, with efficiency and precision, the variation of the free-vibration amplitude of the column as a function of the natural frequency.

From the excellent correlation between numerical and experimental results, it is also concluded that the developed mathematical modeling represents the dynamic behavior of slender columns in a versatile and precise way, for all tested lengths, including post-buckling regimes. Both the experimental results and those obtained by integration of the non-linear equations of motion show that for compressed column lengths higher than 40 cm present a softening behavior not observed in the free vibration of slender beams. It is believed that this behavior is due to the loss of the compressed column stiffness, caused by the simultaneous effect of the self-weight together with the large rotations presented in the free-vibration movement (softening phenomenon), which lead to important inertial non-linearities.

Regarding to the alternative experimental methodology developed in this study, based on the digital image processing techniques and on the DLT method, has proved to be an efficient tool for a precise dynamic analysis of structures that cannot be monitored by conventional sensors.

One of the advantages of the developed computational vision system is the capacity to measure dynamic displacements in several points of the structure with

efficiency and accuracy, allowing in this way a better identification of the structural behavior. Another advantage is related to the low cost of the developed measurement system, as compared to conventional systems and to similar vision systems found in the market.

ACKNOWLEDGEMENTS

The authors wish to thank the National Council for Scientific and Technological Development (CNPQ) and the National Petroleum Agency (ANP) for the financial support and the Laboratory for Experimental Dynamics and Image and Signal Processing (Civil Engineering Program – COPPE / UFRJ) for the infrastructure used to realize this work.

REFERENCES

Abdel-Aziz, Y. I., and Karara, H. M., "Direct linear transformation from comparator coordinates into object space coordinates in close-range photogrammetry." *Proceedings of the Symposium on Close-Range Photogrammetry*, Falls Church, VA: American Society of Photogrammetry, pp. 1-18, 1971.

Anjos, A. M. G., Analysis of the Nonlinear Behavior and the Instability of Slender One-Dimesional Elements. *M.Sc. Dissertation*, Civil Engineering Department, Catholic University, PUC-Rio, Rio de Janeiro, Brazil, 1995.

Braun, M., "On some properties of the multiple pendulum." *Archive of Applied Mechanics*, 72, 899-910, 2003.

Buffoni, S. S. O., Parametric Instability of Columns. *M.Sc. Dissertation*, Civil Engineering Department, Catholic University, PUC-Rio, Rio de Janeiro, Brazil, 1998.

Chirikov, Victor A., "Causes for the softening phenomenon at vibrations of beams undergoing large rotation." *ENOC-2005*, Eindhoven, Netherlands, 2541-2547, 2005.

Clough, R.W., and Penzien, J., Dynamics of Structures. McGraw-Hill, 1993.

Gonçalves, P. B., Jurjo, Daniel L .B. R., Magluta, C., Roitman, N., Pamplona D., "Large Deflection Behavior and Stability of Slender Bars under Self-Weight." *Structural Engineering and Mechanics*, 24, 709-725, 2006.

Haralick, R. M., and Shapiro, L. G., *Computer and Robot Vision 2*, Addison-Wesley Publishing Company, 1993.

Hack, E., and Leroy, D., "Camera-based monitoring of the rigid-body displacement of a mandrel in superconducting cable production." *Optics and Lasers in Engineering*, 43, 455-474, 2005.

Jones, A., Shaw, J., Wineman, A., "An experimental facility to measure the chemorheological response of inflated elastomeric membranes at high temperature." *Experimental Mechanics*, 46, 579-587, 2006.

Jurjo, Daniel L. B. R., Stability of Columns under Self-Weight (in Portuguese). *M.Sc. Dissertation*, Civil Engineering Department, Catholic University, PUC-Rio, Rio de Janeiro, Brazil, 2001.

Jurjo, D.L.B.R., Magluta, C., Roitman, N. and Gonçalves, P.B., "Experimental

Methodology for the Dynamic Analysis of Slenders Structures Based on Digital Image Processing Techniques", *Mechanical Systems and Signal Processing*, Vol. 24, issue 5, pp. 1369-1382, 2010.

Jurjo, Daniel L. B. R., Magluta, C., Roitman, N., Gonçalves, P. B., "Vibration Analysis of Slender Columns Under Self-Weight Using Digital Image Processing Techniques". *Euromech Colloquium 483* (*Geometrically Non-linear Vibrations of Structures*), Porto, Portugal, 2007.

Jurjo, Daniel L. B. R., Development of a Computer-Based Vision System for Measuring Displacements in Structures (in Portuguese). *PhD. Thesis*, Civil Engineering Department, COPPE/UFRJ, Rio de Janeiro, Brazil, 2007.

Jurjo, Daniel L. B. R., Magluta, C., Roitman, N., Gonçalves, P.B., "Dynamic analysis of slender columns under self-weight using digital image processing techniques." *Proceedings of the 18th International Congress of Mechanical Engineering*, 2005.

Lee, B. K., Wilson, J. F., Oh, S. J., "Elastica of cantilevered beams with variable cross sections." *International Journal of Non-linear Mechanics*, v. 28, pp. 579-589, 1993.

Lee, J. J., and Shinozuka, M., "Real- time displacement measurement of a flexible bridge using digital image processing techniques." *Experimental Mechanics*, 46, 105-144, 2006a.

Lee, J. J., Shinozuka, M., "A Vision-Based System for Remote Sensing of Bridge Displacement." *NDT & E International*, v.39, pp. 425-431, 2006b.

Maia, N. M. M., *Introdução á Dinâmica Analítica (Introduction to Analytical Dynamics)*. IST Press, 2000.

Pamplona, D., Gonçalves, P. B., Davidovich, M., Weber, H. I., "Finite axisymmetric deformations of an initially stressed fluid-filled cylindrical membrane." *Int. J. of Solids and Structures*, v. 38, pp. 2033-2047, 2001.

Sathyamoorthy, M., *Nonlinear Analysis of Structures*. CRC Press, New York, 1998.

Virgin, L.N. and Plaut, R.H., "Postbuckling and vibration of linearly elastic and softening columns under self-weight", *Int. J. Solids Struct*., 41, 4989-5001, 2004.

Wang, C. Y., "Buckling and post-buckling of a long-hanging elastic column due to a bottom load." *Journal of Applied Mechanics*, ASME, v. 50, pp. 311-314, 1983.

Yoneyama, S., Morimoto, Y., Fujigaki, M., Ikeda, Y., "Scanning Moiré and spatial-offset phase-stepping for surface inspection of strucutures." *Optics and Lasers in Engineering*, 43, 659-670, 2005.